

# Effects of Gaussian beam radius on the conversion efficiency and the diffusion capacitance of a polycrystalline silicon solar cell

Comment [G1]: Inserted: G

Comment [G2]: Deleted:g

## Abstract

This study presents effects of Gaussian beam radius ( $r_f$ ) on the power and the conversion efficiency ( $\eta$ ) of a polycrystalline silicon solar cell. The two-dimensional continuity equation solved using finite element method, permits to determine the excess minority carriers density, the photocurrent density and the photo voltage from which the power and the conversion efficiency of the solar cell are calculated. The capacitance (C) and the space charge region (SCR) width are also examined for various values of the radius of gaussian luminous flow. The gaussian luminous flow effects on solar cell's performances are highlighted in comparing with those of a classical monochromatic illumination.

Comment [G3]: Inserted: G

Comment [G4]: Deleted:g

Comment [G5]: Deleted:s

**Keywords:** solar cell, gaussian flow, conversion efficiency, capacitance, space charge region, recombination velocity.

## I. Introduction

Solar cells, generally designed to be illuminated by solar light, have an absorption spectrum of which wavelengths extend from 300 to 1100 nm [1,2]. Thus, to improve their performances, several studies have been carried out, by subjecting them to various types of illuminations such as laser beams [2-4]. These studies have permitted to determine solar cell electrical parameters, namely, the current-voltage characteristic, series resistance, and shunt resistance, as well as the diffusion length, when it is illuminated by a Gaussian luminous flow [1-4]. These studies for most of the cases have not taken into account the solar cell power and its conversion efficiency.

Comment [G6]: Inserted: ,

Comment [G7]: Deleted: ,

Comment [G8]: Inserted: m

Comment [G9]: Inserted: a

Comment [G10]: Inserted: G

Comment [G11]: Deleted:e aim of th

Comment [G12]: Deleted:g

Comment [G13]: Deleted: on

This study aims to determine the effects of the Gaussian luminous flow radius on the power and the conversion efficiency of a polycrystalline silicon solar cell, on its diffusion capacitance and the charge space region extension, using a finite element method [2][4-8].

The power and the conversion efficiency of the solar cell will be determined for various values of gaussian beam radius, as well as the diffusion capacitance, and the space charge region (SCR) extension of the solar cell.

After solving the continuity equation using this method, we will determine the excess minority carriers density [9-10], and a comparative study will be done when the solar cell is illuminated respectively by a classical monochromatic flow, and by a Gaussian luminous beam.

42 **II. Theoretical approach**

43

44 **II.1 Continuity Equation**

45 Let us consider a polycrystalline silicon solar cell, constituted by an emitter doped n-type  
 46 with a weak thickness and a base doped p-type with a depth  $H_1$  according to x and a width  $H_2$   
 47 according to y, as represented in figure 1. When the solar cell is not illuminated, between the  
 48 emitter and the base there is a depletion region called space charge region (SCR) inside  
 49 which the internal electric field  $\vec{E}$ , as opposed to the diffusion of the majority carriers A  
 50 width  $W$  and a capacitance  $C_0$ , characterizes this region. When the solar cell is illuminated,  
 51 the excess minority carriers photogenerated diffuse towards the space charge region i.e. the  
 52 electrons of the base and holes of the emitter. The charge carriers reach the space charge  
 53 region are accelerated by the internal electric field, thus creating a diffusion photocurrent  
 54 [11].

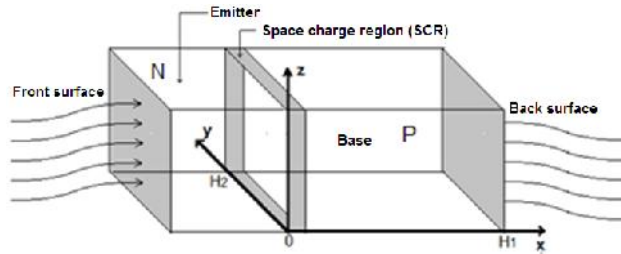


Figure 1 : Crystal of a bifacial silicon solar cell

55

56

57

58 In this study, we neglect the current contribution of the emitter into the photocurrent and the  
 59 height of solar cell along the z-axis [9]. Thus the continuity equation which governs the solar  
 60 cell operation is given by [4, 12, 13]:

61 
$$\frac{\partial^2 \delta(x,y)}{\partial x^2} + \frac{\partial^2 \delta(x,y)}{\partial y^2} - \frac{\delta(x,y)}{L^2} = -\frac{g(x,y)}{D} \quad (1)$$

62  $(x, y)$  represents the excess minority carriers density, i.e., the electrons in the base P.  $x$  and  $y$   
 63 are the coordinates related to the base depth and the solar cell width respectively.  $L$  and  $D$   
 64 indicate respectively, the diffusion length and the diffusion coefficient of the electrons, and  
 65  $g(x, y)$ , its generation rate.

66 When the solar cell is illuminated on its front surface, this generation rate is given by [2, 4, 6,  
 67 14] :

68

69 
$$g(x, y) = \begin{cases} I_0(1 - R) \exp(-\alpha x) & \text{for a classical monochromatic flow (2 a)} \\ I_0(1 - R) \frac{\alpha}{2\pi r_f^2} \exp(-\alpha x) \cdot \exp\left(-\frac{y^2}{2r_f^2}\right) & \text{for a gaussian luminous flow (2 b)} \end{cases}$$

70  $I_0$  is the incidental beam of photons.  $\alpha$  and  $R$  represent respectively, the absorption coefficient  
 71 and the reflection coefficient of the solar cell and  $r_f$ , the radius of gaussian luminous beam.

72 This continuity equation obeys to the following boundary conditions relating to the  
 73 conservation of the diffusion current and the recombination current on the boundaries of the  
 74 solar cell [2, 6]:

75 - on the junction

76

Comment [G14]: Inserted: a  
 Comment [G15]: Inserted: ,  
 Comment [G18]: Deleted: i  
 Comment [G16]: Inserted: A  
 Comment [G17]: Inserted: , characterizes this region  
 Comment [G19]: Deleted: This region is characterized by a

77 
$$\left. \frac{\partial \delta(x,y)}{\partial x} \right|_{x=0} = \frac{S_j}{D} \cdot \delta(0,y) \quad (3)$$

78 - on the back surface

79  
80 
$$\left. \frac{\partial \delta(x,y)}{\partial x} \right|_{x=H_1} = -\frac{S_b}{D} \cdot \delta(H_1,y) \quad (4)$$

81 - on the y=0 boundary

82  
83 
$$\left. \frac{\partial \delta(x,y)}{\partial x} \right|_{y=0} = \frac{S_{bg}}{D} \cdot \delta(x,0) \quad (5)$$

84 - and on the y=H<sub>2</sub> boundary

85  
86 
$$\left. \frac{\partial \delta(x,y)}{\partial x} \right|_{y=H_2} = -\frac{S_{bg}}{D} \cdot \delta(x,H_2) \quad (6)$$

87 S<sub>j</sub> indicates the junction recombination velocity, S<sub>b</sub> the back surface recombination velocity  
88 and S<sub>bg</sub>, the boundary recombination velocity on the boundaries y=0 and y=H<sub>2</sub>.

89 Knowing the photo generated minority charge carriers density, the photocurrent density and  
90 the photo voltage are calculated from the following relations (7) and (8) :

91  
92 
$$J = \frac{q \cdot D}{H_2} \int_0^{H_2} \left[ \frac{\partial \delta(x,y)}{\partial x} \right]_{x=0} dy \quad (7)$$

93  
94 
$$V = V_T \cdot \text{Log} \left( \frac{N_b}{n_i^2} \int_0^{H_2} \delta(0,y) dy + 1 \right) \quad (8)$$

95 where V<sub>T</sub> represents the thermal voltage, N<sub>b</sub>, the base doping level and n<sub>i</sub>, the silicon intrinsic  
96 carrier's density of the silicon.

97 Knowing the photocurrent density values and those of the photo voltage, one can easily  
98 calculate the power P provided by the solar cell:

99 
$$P = VJA \quad (9)$$

100 where A is the solar cell's surface.

## 101 **II.2 Solar cell conversion efficiency**

102  
103 An important parameter in the solar cells characterization is the conversion efficiency given  
104 by the relation (10) [15-16]:

105 
$$\eta = \frac{P_m}{P_{inc}} = \frac{V_m I_m}{P_{inc}} \quad (10)$$

106 where P<sub>m</sub> indicates the optimal solar cell power and P<sub>inc</sub>. i.e, the incidental power. V<sub>m</sub> and  
107 I<sub>m</sub> are respectively, photo voltage and the photocurrent corresponding to the optimal power  
108 P<sub>m</sub>.

109  
110 Another interesting parameter is the fill factor which permits to evaluate the quality of a solar  
111 cell or a photovoltaic generator. The higher it is, the more exploitable power provided by the  
112 solar cell is important. It is given by the relation (16):

Comment [G20]: Inserted: ing

113  
114  
115  
116

$$FF = \frac{V_{oc} I_m}{V_{oc} I_{sc}} \quad (11)$$

$V_{oc}$ , indicates the open circuit photo voltage and  $I_{sc}$  the short-circuit photocurrent.

### 117 **II.3 Diffusion capacitance and space charge region width**

118 The diffusion capacitance of the solar cell is due to the diffusion of excess minority charge  
119 carriers through the junction. It can be determined by the relation (12) [17, 18].

$$120 \quad C = \frac{dQ}{dV} = \frac{q n l^2}{V_T} \exp\left(\frac{V}{V_T}\right) \quad (12)$$

121 This diffusion capacitance is composed of two terms: one term related to the intrinsic  
122 capacitance and another term which depends on the solar cell operating point and thus on the  
123 junction recombination velocity  $S_j$  [19]. It is related to the space charge region width  $X_p$  by  
124 the relation [17, 18]:

$$125 \quad C = \frac{A \epsilon_0 \epsilon_r}{X_p} \quad (13)$$

126 where  $A$  indicates solar cell surface,  $\epsilon_0$ , vacuum's dielectric permittivity and  $\epsilon_r$ , the relative  
127 permittivity of silicon.

128

## 129 **III. Results and Discussions**

130 The continuity equation (1), which is solved using the finite element method computer code  
131 that we have conceived, permits to determine the photo generated minority charge carriers  
132 density from which the others quantities can be calculated by the relations (7-13).

133 To highlight effects of gaussian beam radius  $r_f$  on the improvement of the conversion  
134 efficiency and on the diffusion capacitance of the solar cell, we have determined these  
135 quantities for various values of  $r_f$ , with a grain boundaries recombination velocity  $S_{bg} =$   
136  $10^2 \text{ cm/s}$  and an incidental power  $P_{inc} = 100 \text{ mW/cm}^2$ .

137 In addition, when the silicon solar cell is illuminated by a gaussian luminous flow, the  
138 variation of the generation rate according to the wavelength  $\lambda$  shows that this one is maximum  
139 around a value of  $\lambda = 800 \text{ nm}$ . For this wavelength of illumination, the corresponding  
140 reflexion coefficient and absorption coefficient are  $R = 0,3448$  and  $\alpha = 825,8 \text{ cm}^{-1}$  [2,  
141 4].

142

### 143 **III.1 Solar cell Power**

144 In Figure 2, we represented the power of the solar cell versus the junction recombination  
145 velocity  $S_j$  and the grain width  $y$ , when the solar cell is illuminated on its front surface, by a  
146 gaussian luminous flow.

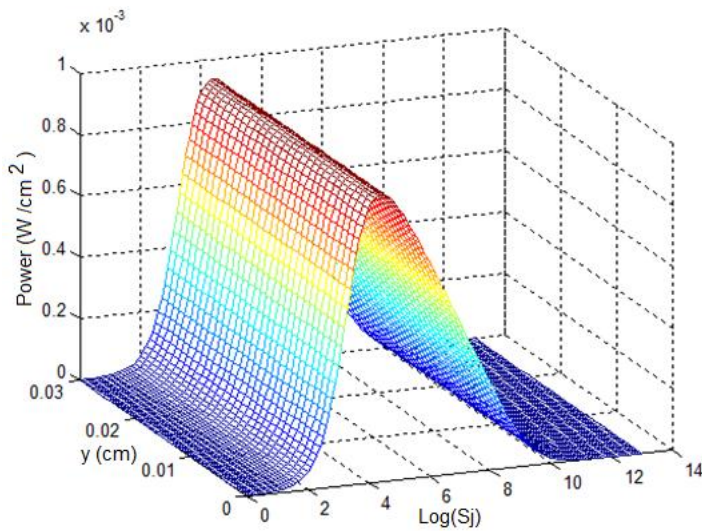


Figure 2 : Solar cell power versus  $S_j$  and  $y$

147  
148

149 As waited, the solar cell power increases according to  $S_j$ , reaches a maximum value  
150 corresponding to the optimal power  $P_{m,s}$ , then decreases and cancels out, when  $S_j$  becomes  
151 very great.

152 In Figure 3, we illustrated the solar cell power when it is illuminated by a gaussian luminous  
153 flow and a monochromatic luminous flow.

154

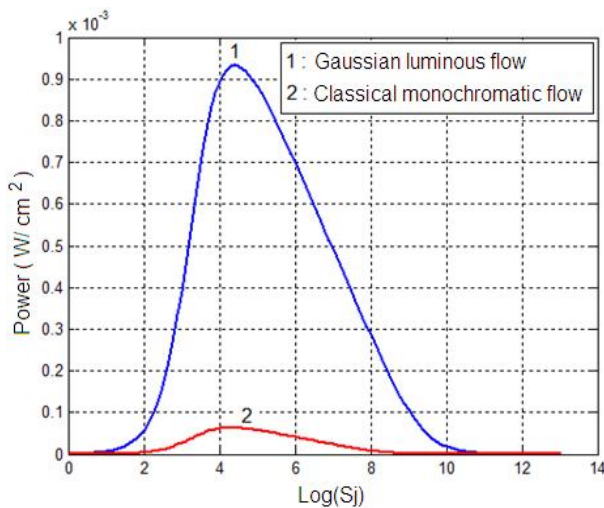
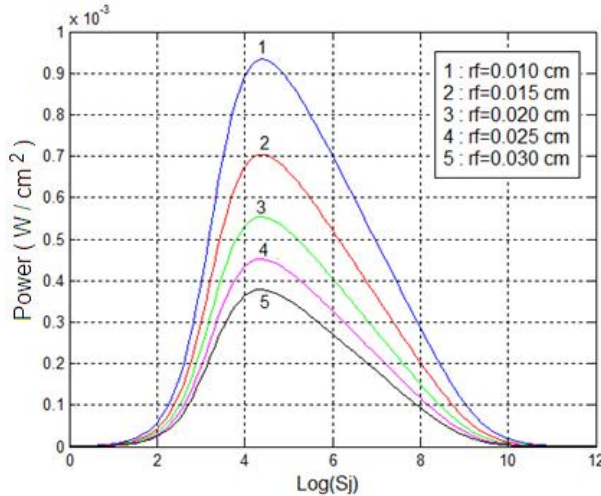


Figure 3 : Solar cell power versus  $S_j$  : gaussian and classical monochromatic flow

155  
156

157 As waited, this power is higher when the solar cell is illuminated by a gaussian luminous  
158 flow. In fact, for this illumination, the carriers generation phenomenon is more important. To

159 illustrate the effects of the gaussian beam radius, we have represented the power of the solar  
 160 cell in figure 4, for various values of  $r_f$ , versus the junction recombination velocity  $S_j$ .



161  
 162 **Figure 4 : Solar cell power**

163 We can note that the gaussian beam radius has a considerable effect on the power of the solar  
 164 cell. The weaker it is, the more the solar cell power is important, because the reduction of the  
 165 gaussian beam radius led to the increase in the incidental power per unit of area since  
 166 incidental flow  $I_0$  is constant.

167  
 168 **III.2 Conversion efficiency and fill factor of the solar cell**

169 Using our matlab code for various values of  $r_f$ , with  $S_b = 10^2 \text{ cm/s}$ ,  $S_{bg} = 10^2 \text{ cm/s}$  and  
 170  $S_j = 3.9811 \cdot 10^4 \text{ cm/s}$ , corresponding to the optimal operating point of the solar cell. we  
 171 have determined the optimal photo voltage  $V_m$ , the optimal photo current density  $J_m$ , the  
 172 optimal power  $P_m$ , the short-circuit photocurrent density  $J_{cc}$  and the open circuit photo  
 173 voltage  $V_{co}$ . The conversion efficiency of the solar cell, its fill factor  $FF$ , conversion  
 174 efficiency  $\eta$  can be easily calculated starting from the above relations (7-13). The results  
 175 obtained are given in table 1

176  
 177 **Table 1 : Conversion efficiency and fill factor of the solar cell**  
 178

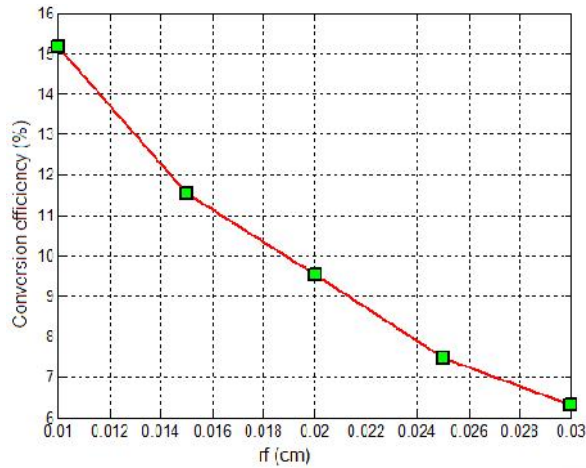
$r_f$ (cm)	$V_m$ (V)	$J_m$ (mA)	$P_m$ (mW)	$J_{cc}$ (mA)	$V_{co}$ (V)	$FF$	$\frac{P_m}{J_m V_{co}}$ (%)	$PF :$ $S_j$ (cm/s)
0.010	0.4596	3.2979	1.5160	3.5302	0.5374	0.7989	15.160	$3.9811 \cdot 10^4$
0.015	0.4529	2.5454	1.1528	2.7198	0.5308	0.7985	11.530	$3.9811 \cdot 10^4$
0.020	0.4472	2.0422	0.9536	2.1810	0.5251	0.7976	09.536	$3.9811 \cdot 10^4$
0.025	0.4423	1.6926	0.7487	1.8070	0.5203	0.7966	07.487	$3.9811 \cdot 10^4$
0.030	0.4382	1.4377	0.6308	1.5360	0.5161	0.7956	06.308	$3.9811 \cdot 10^4$

179  
 180 One can note that at the optimal operating point of the solar cell, the gaussian beam radius  $r_f$   
 181 has a significant effect on the conversion efficiency as shown in figure 5. , where  $\eta$  is

Comment [G21]: Inserted: g  
 Comment [G22]: Deleted.t



182 represented according to  $r_f$ . On the other hand the variation of the gaussian beam radius does  
183 not seem to influence the fill factor of the solar cell.  
184

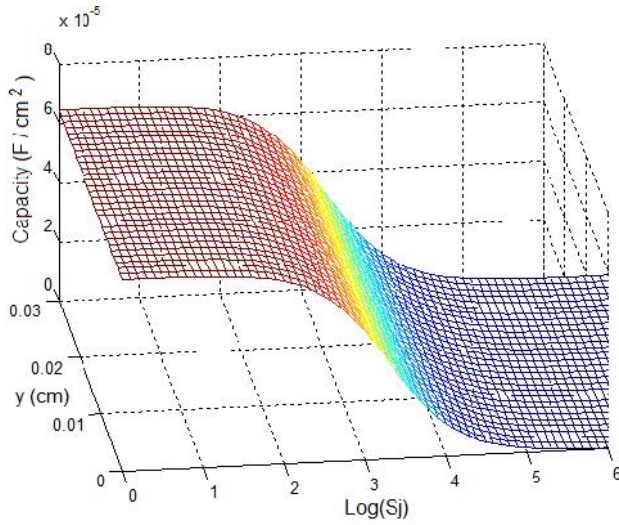


185  
186 **Figure 5 : Conversion efficiency versus gaussian beam radius**

187 The conversion efficiency increases with the reduction of the gaussian beam radius, owing to  
188 the increase in the optimal power which is directly related to  $P_m$  and  $J_m$ . In the same way,  
189  $J_{CC}$  and  $V_{CO}$  are more important when  $r_f$  is weak. This conversion efficiency which reaches  
190 the value of 15% for  $rf = 0.01cm$ , is definitely better than the conversion efficiency of 12%  
191 or 13% obtained for polycrystalline solar cells subjected to usual solar illuminations [20].

### 192 **III.3 Diffusion Capacitance**

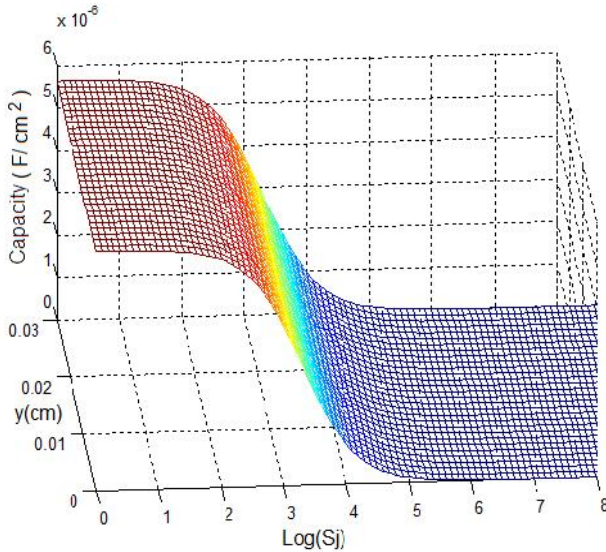
193 We were also interested in the behavior of the diffusion capacitance of the solar cell when it  
194 is illuminated on its front surface by a gaussian luminous flow. It is represented in 2D in  
195 figure 6, according to the junction recombination velocity  $S_j$  and the width  $y$  of the grain of  
196 the solar cell.



197 **Figure 6 : Diffusion capacitance versus  $S_j$  and the grain width  $y$  of the solar cell illuminated by a gaussian**  
 198 **luminous flow**  
 199

197  
 198  
 199

200 In the same way, when we illuminate the solar cell by a classical monochromatic flow, one  
 201 obtains a diffusion capacitance as represented in figure 7.



202 **Figure 7 : Diffusion capacitance versus  $S_j$  and the grain width  $y$  of the solar cell illuminated by**  
 203 **monochromatic luminous flow**  
 204

202  
 203  
 204

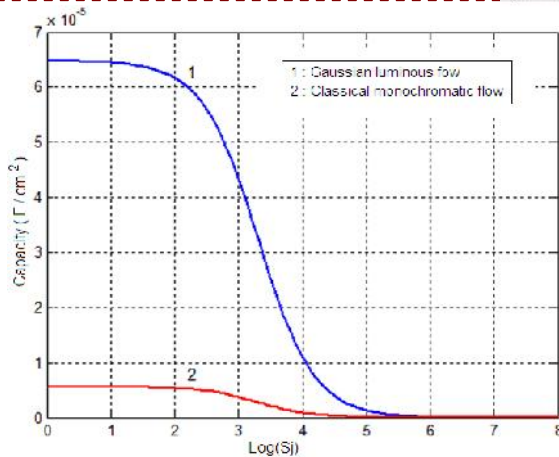
205 One can note that the capacitance of the solar cell decreases according to the junction  
 206 recombination velocity  $S_j$ . For the weak values of  $S_j$ , i.e. in the vicinity of the open circuit, it  
 207 corresponds to the open circuit capacitance  $C_{CO}$ . It is null for the great values of  $S_j$ ,  
 208 corresponding to a short-circuit operation. One also can note that the grain width of the solar  
 209 cell has not effects on the capacitance, whether a gaussian luminous flow illuminates the  
 210 solar cell or not.

210

- Comment [G41]: Deleted:a
- Comment [G23]: Inserted: the
- Comment [G24]: Inserted: s
- Comment [G25]: Inserted: flow
- Comment [G26]: Inserted: nou
- Comment [G27]: Inserted: um
- Comment [G28]: Inserted: n
- Comment [G29]: Inserted: i
- Comment [G30]: Inserted: gaus
- Comment [G31]: Inserted: a
- Comment [G32]: Inserted: ol
- Comment [G33]: Inserted: ce
- Comment [G34]: Inserted: r
- Comment [G35]: Deleted:the
- Comment [G36]: Deleted:ol
- Comment [G37]: Deleted:r
- Comment [G38]: Deleted:ce
- Comment [G39]: Deleted:l
- Comment [G40]: Deleted:d by
- Comment [G42]: Deleted:gau
- Comment [G43]: Deleted:si
- Comment [G44]: Deleted:n
- Comment [G45]: Deleted:uminous f
- Comment [G46]: Deleted:ow



211 To compare the diffusion capacitance of the solar cell illuminated by a gaussian luminous  
 212 flow and what obtained when a classical monochromatic luminous flow illuminates it, we  
 213 have represented in figure 8, both capacitances according to  $S_j$ , for  $r_f = 0.01 \text{ cm}$ .



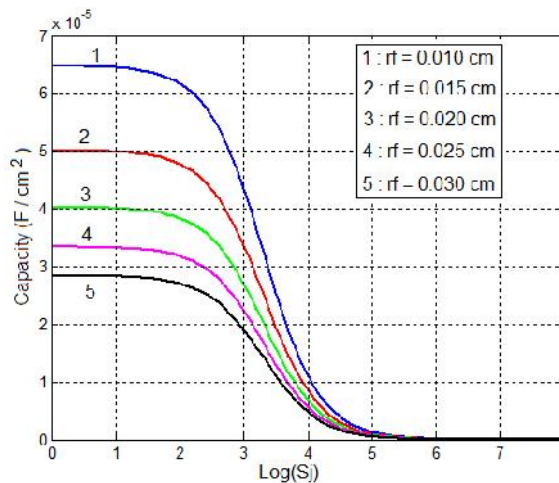
Comment [G47]: Inserted: illuminates it  
 Comment [G48]: Deleted: it is illuminated by

214  
 215 **Figure 8 : Diffusion capacitance for a classical monochromatic flow and a gaussian luminous flow versus  $S_j$**   
 216

217 The diffusion capacitance is more important when the solar cell is illuminated by a gaussian  
 218 luminous flow than when a classical monochromatic flow illuminates it. The photogenerated  
 219 charge carriers density being more important when the solar cell is illuminated by a gaussian  
 220 luminous flow [2], the diffusion of the charge carriers at the junction is also more important.  
 221 That leads to the increase in the diffusion capacitance.

Comment [G49]: Inserted: illuminates it  
 Comment [G50]: Deleted: it is illuminated by

222 One can also note that the effects of the gaussian beam radius on the diffusion capacitance are  
 223 more important on the open circuit diffusion capacitance and decreases with the increase of  
 224  $r_f$ . These effects are illustrated in figure 9.



225  
 226 **Figure 9 : Diffusion capacitance for various values of  $r_f$  versus junction recombination velocity  $S_j$**   
 227

225  
 226  
 227

228

229

### 230 III.4 Space charge region

231 Just like the diffusion capacitance, we have represented in figure 10 for a value of  $r_f =$   
232  $0.01 \text{ cm}$ , when the solar cell is illuminated by a gaussian luminous flow and by a classical  
233 monochromatic flow.

234 To examine the effects of gaussian beam radius on the widening of the space charge region,  
235 we represented it for various values of  $r_f$ . These curves are given in figure 10.  
236

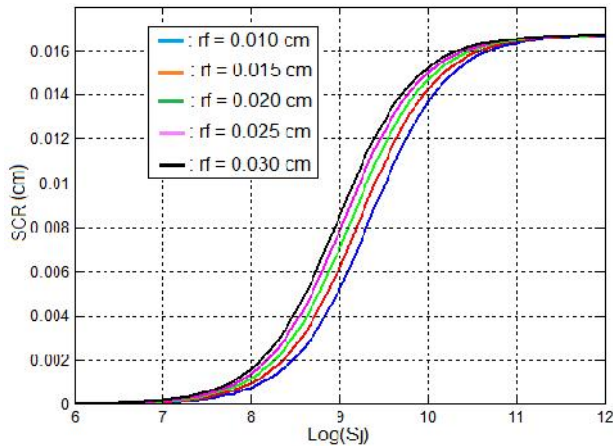


Figure 10 : Width of space charge region for various values of  $r_f$

237  
238

239 When one vary the gaussian beam flow, the profile of the width of the space charge region  
240 according to  $S_j$  is practically the same one and the saturation value is the same one for the  
241 various curves. In general, one can note that the gaussian beam radius has an effect limited on  
242 the width of the space charge region.

243

### 244 IV. Conclusion

245 After determining the charge carriers density by solving the continuity equation using finite  
246 element method from which the photocurrent density and the photo voltage of solar cell were  
247 deduced, the effects of gaussian beam radius on the power and the conversion efficiency of  
248 the cell have been highlighted. These effects are more remarkable on the capacitance of the  
249 solar cell than on the width of the space charge region. One also can note that the grain width  
250 of the solar cell does not have effects on the diffusion capacitance and the space charge  
251 region width.

252 Thus, from this study, we can note that compared with a classical monochromatic  
253 illumination, the gaussian luminous flow has considerable effects on the solar cell electrical  
254 parameters. These effects are characterized by the improvement of the solar cell  
255 performances, owing to the reduction of the gaussian beam radius leading to the increase in  
256 the solar cell conversion efficiency.

257

258

259  
260

261 **Références**

- 262 1. Yassine SAYAD Détermination de la longueur de diffusion des porteurs dans le silicium  
263 cristallin par interaction lumière matière, Thèse de Doctorat, 2009, Institut National des  
264 Sciences Appliquées de Lyon, France.
- 265 2. Nzonzolo, Contribution to the Caractération of a Photopile Polycristalline and Silicium on  
266 the Meteorite des Eléments Finis, Thèse de Doctorat, 2017, Université Marien NGOUABI,  
267 Congo.
- 268 3. Syad Yassine, Interaction Laser-Semi-conducteur: Contribution of the University of LBIC  
269 - Application of a photocoltaic application, Thèse de doctorat, 2009, Université Mentouri  
270 Constantine Faculty of Sciences Exertes Département de Physique, Algérie.
- 271 4. Nzonzolo, D. Lilonga-Boyenga, Beam radius effects on polycrystalline bifacial silicon  
272 solar cell electrical parameters, 2017, Journal of Scientific and Engineering Research JSAER,  
273 4(5), 143-146.
- 274 5. Nzonzolo, Desire Lilonga-Boyenga, Camille N. Mabika and Gregoire Sissoko,  
275 Characterization of a Bifacial Silicon Solar Cell Under Multispectral Steady State  
276 Illumination Using Finite Element Method, Progress In Electromagnetics Research M,  
277 2017, Vol. 53, 131–140,
- 278 6. Nzonzolo, Désiré Lilonga-Boyenga, Camille Nziengui Mabika, Grégoire Sissoko, Two-  
279 Dimensional Finite Element Method Analysis Effect of the Recombination Velocity at the  
280 Grain Boundaries on the Characteristics of a Polycrystalline Silicon Solar Cell, Circuits and  
281 Systems, 2016, 7, 4186-4200 (Scientific Research Publishing).
- 282 7. A. Dieng, N. Thiam, ML Samb, AS Maiga, FI Barro, G. Sissoko, Etude à 3D d'une  
283 Photopile Polycristalline au Silicium: Influence de la taille de grain de la vitesse de  
284 recombinaison aux joints des grains sur les paramètres électriques, 2009, Journal des  
285 Sciences, J. Sci. Vol. 9, N° 1, 51 - 63.
- 286 8. M. Diaw, B. Zouma, A. Sere, S. Mbodji, A. Gueye Camara, G. Sissoko, 3D study to  
287 improve the IQE of the bifacial polycrystalline silicon solar cell from the grain's geometries  
288 and the applied magnetic field, 2012, International Journal of Engineering Science and  
289 Technology (IJEST), Vol. 4 No.08,p. 3673-3682.
- 290 9. Tao J., Cours Méthodes Numériques en Physiques Appliquées, Institut National  
291 Polytechnique de Toulouse, Université de Toulouse, France
- 292 10. Matthew N. O. Sadiku, Numerical Techniques in Electromagnetics (Second Edition)  
293 CRC Press LLC, Boca Raton London, New York , Washington, D.C, 2001

- 294 11. Henry Mathieu, Hervé Fanet, Dispositif semiconducteurs et composantes électroniques,  
295 6e édition, Dunod Paris 2009, ISBN 978-2-10-051643-8.
- 296 12. Sze S. M., Physics and Semiconductors devices, Second Edition, Bell Laboratory  
297 Incorporated Murray Hill New Jersey, 2001.
- 298 13. Sze S. M., Semiconductor Devices Physics and Technology, 2nd Edition, ISBN 0-471-  
299 33372-7, Library of Congress Cataloging in Publication Data, United States of America,  
300 2002.
- 301 14. Sze S. M., Kwok K. N., Physics of Semiconductor Devices, 3rd edition, WILEY  
302 INTERSCIENCE, New Jersey, 2006.
- 303 15. Emmanuel Nanema, Modélisation d'une photopile bifaciale au silicium: Méthodes de  
304 détermination des paramètres des paramètres de recombinaison, The Doctorat troisième  
305 cycle, 1996, Université Cheikh Anta Diop, Dakar Sénégal.
- 306 16. Helali KAMELIA: Modélisation d'une cellule photovoltaïque Etude comparative,  
307 Mémoire de Magister en électrotechnique, Université MOULOUD MAMMARI de TZI-  
308 OUZOU, Faculté de Génie Electrique et Informatique, 2012, Algérie.
- 309 17. Saïdou MADOUYOU, Détermination des paramètres électriques d'une photopile bifaciale  
310 au silicium en régime static éclairé multispectral constant et sous l'effet d'une  
311 chiméante, Thèse de Doctorat 3e cycle, 2004, Faculté des Sciences et Techniques Université  
312 Cheikh Anta Diop Dakar Sénégal
- 313 18. Biram DENG, a translation of a photopile bipassiale and silicium in a ceramics at the  
314 University of Aurelian University, in Thèse de Doctorat 3e cycle, 2002, Faculté des  
315 Sciences and Techniques Université Cheikh Anta Diop, Dakar Sénégal.
- 316 19. M.A. Ould El Moujtaba, M. Ndiaye, A. Diao, M. Thiame, I.F. Barro and G. Sissoko,  
317 Theoretical Study of the Influence of Irradiation on a Silicon Solar Cell Under, Multispectral  
318 Illumination, Research Journal of Applied Sciences, Engineering and Technology, 4(23):  
319 2012, 5068-5073.
- 320 20. Laradji-Toumouh Nawal, Etude des Photopiles Solaris nanostructures base de Nitrites  
321 III-V: GaN, AlN, InN, Mémoire, for a Diploma of Diploma, 2012, Ecole Doctorale  
322 Nanosciences, Nanotechnologie, Nanométrie, Université d'Oran, Algérie.